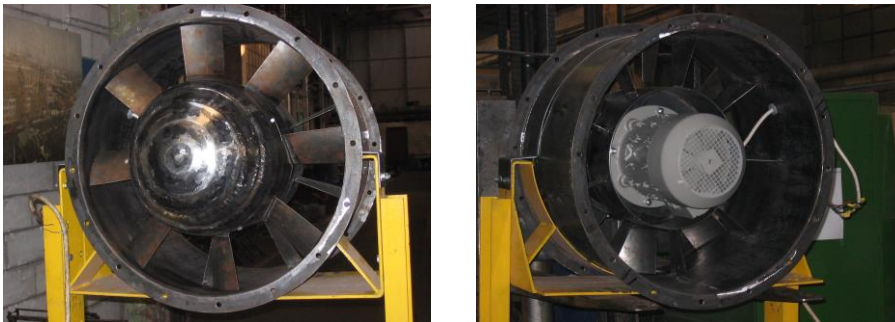## 2. AXIAL FLOW FANS

### 2.1. Construction



**Fig. 2.1. The prototype of the axial fan of high throwing distance (used in fog cannons) with sheet metal blades and bluff hub nose. Developed at the Department of Fluid Mechanics, Budapest University of Technology and Economics.**
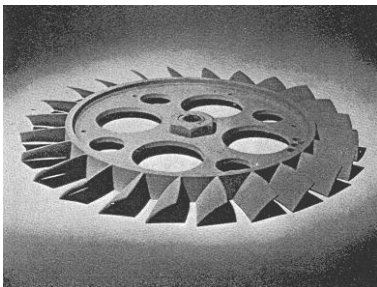


**Fig. 2.2. The above fan with hemispherical nose cone. Front and rear views (direct drive, outlet guide vanes)**
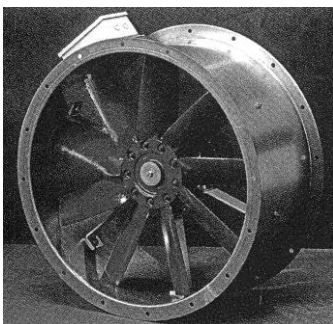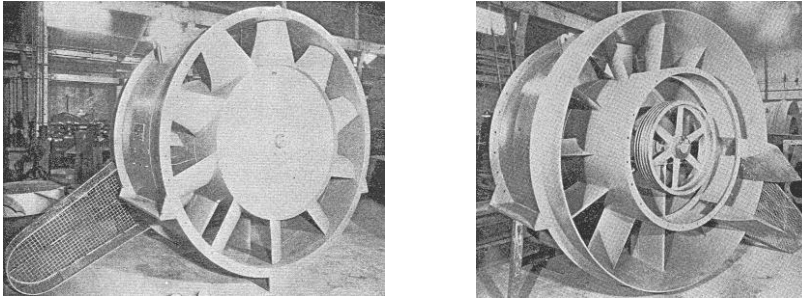


**Fig. 2.3. During tests**
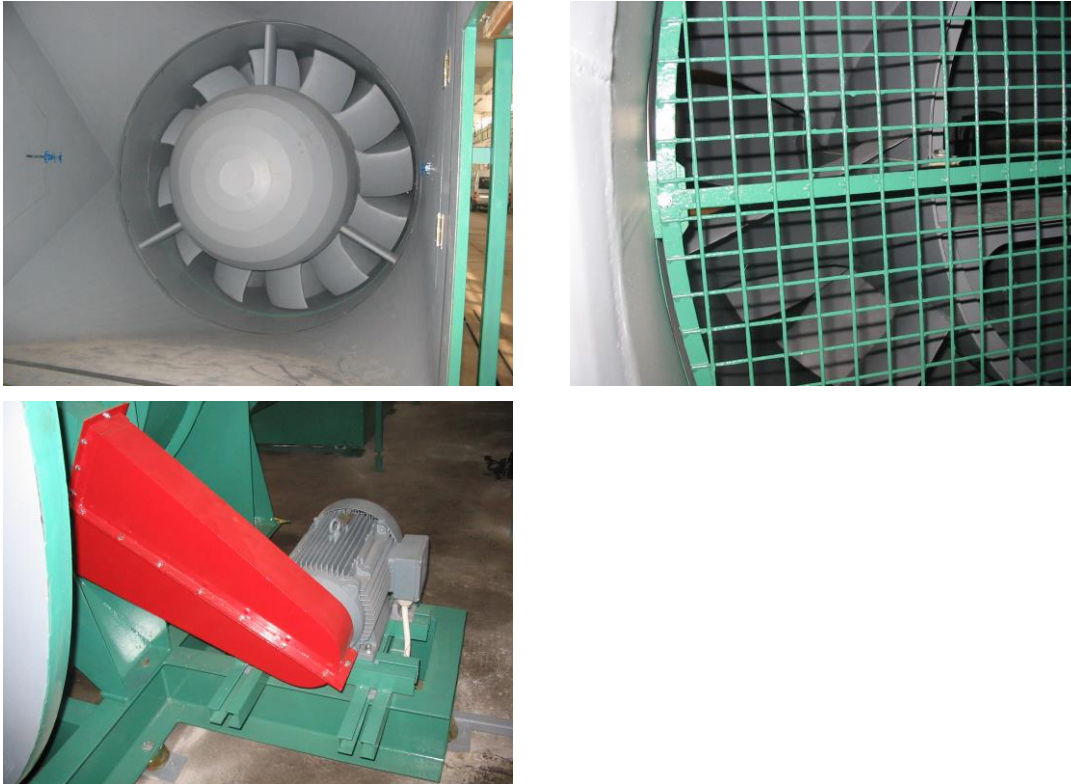
***Fig. 2.4. Rotor of wind tunnel fan developed by the Department of Fluid Mechanics, Budapest University of Technology and Economics. Hemispherical nose cone, profiled blading, outlet guide vane, wedge belt drive.***
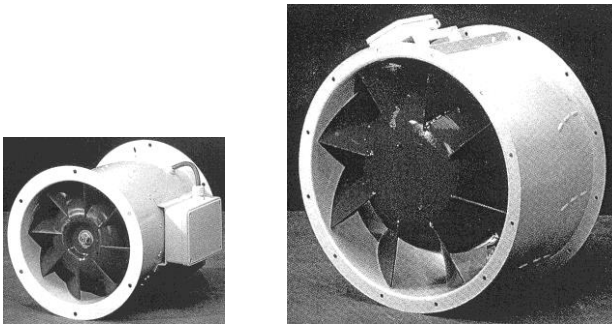


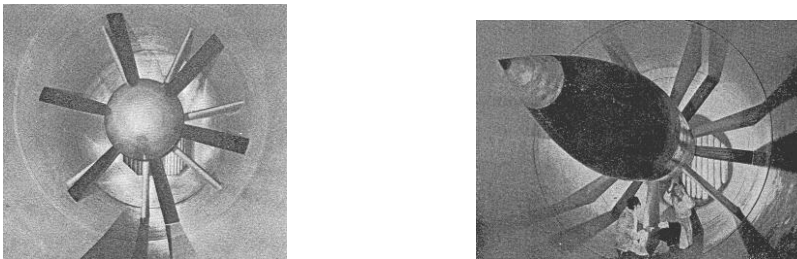***Fig. 2.5. Rotor with plate blades [10]***



***Fig. 2.6. Fan with profile blades of adjustable stagger angle. No guide vanes [6]***
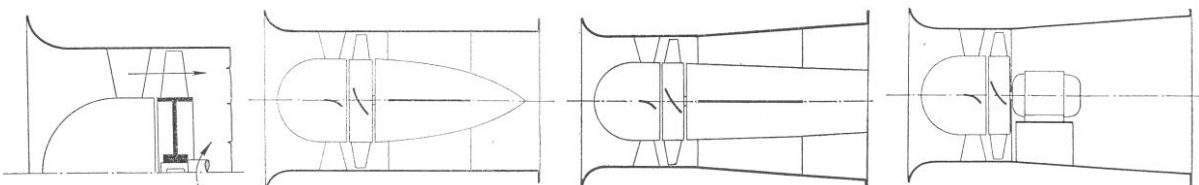
**Fig. 2.7. Industrial fan. Outlet guide vanes, indirect drive [10]**



**Fig. 2.8.  HELIOS RADAX VAR 400 and 1000 [6]**



**Fig. 2.9. Wind tunnel fan with special nose cone and hub diffuser [10]**



**Fig. 2.10. Arrangement with inlet guide vanes and no outlet diffuser; with hub diffuser; with outer and hub diffuser; with outer diffuser and no hub diffuser [2]**

- Plate (sheet metal) blades – Profile blades

- No guide vanes – Inlet or outlet guide vanes (IGV, OGV)

- With nose cone (rotating or steady) – Without nose cone

- With tip clearance – Without tip clearance

- Direct – Indirect drive

- Without outlet diffuser – With hub diffuser and / or outer diffuser

Nose cone: of ellipsoid profile in ideal case (accelerating flow with moderate separation), but is manufactured as a hemisphere in several cases. Steady nose cone: may be fitted to the duct with use of the inlet guide vane. Nose cone: 1 – 2 % gain in efficiency. IGV: plate blading in the case of fans of moderate size. OGV: frequently formed from the motor support ribs. Motor

support rib: may act as an OGV if inclined to the flow in an appropriate manner. OGV: use of plate blades is to be avoided, if noise minimisation is an important issue (flow separation). Distance between rotor and guide vanes: at least 1 rotor blade pitch (to reduce interaction noise and pulsating mechanical load).

In general: profile blades instead of plate blades:

- Fluid mechanical reasons (various operating points: the stagnation point can wander on the curved blade leading edge: reduced separation losses)

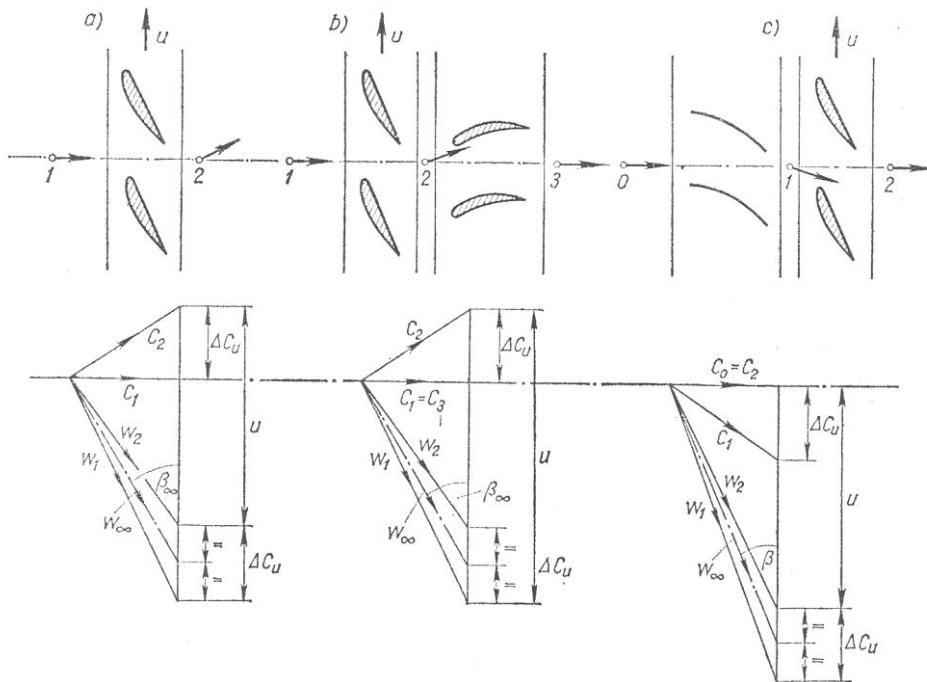- Structural reasons (mechanical strength)

## 2.2. Operation of various arrangements

Euler equation of turbomachines:

$$\Delta p_{tid} = \rho\left(\underline{c}_2\underline{u}_2 - \underline{c}_1\underline{u}_1\right) \tag{1.9}$$

Here, $r_1 \approx r_2$ , $u_1 \approx u_2$, and therefore

$$\Delta p_{tid} = \rho u(c_{2u} - c_{1u}) = \rho u \Delta c_u \tag{2.1}$$



***Fig. 2.11. Velocity diagrams for a/ No guide vanes, b/ OGV, c/ IGV [2]***

Disadvantage of vaneless fans: swirling outlet jet, waste of kinetic energy (may be up to 10 % of the useful power). The guide vanes also generate loss, but if this loss is considerably lower than the swirl loss, the application of the guide vane may be reasonable. Guide vanes: at high performances, or when the divergence of the outflow is to be minimised.

Application of either IGV or OGV may depend on design aspects, and expenses.

The velocity triangles of the rotor are specific to the operation of the guide vanes.

For no guide vane (a/) and OGV (b/) cases:

$$w_\infty^2 = c_a^2 + \left(u - \frac{\Delta c_u}{2}\right)^2 \tag{2.2a}$$

and

$$\beta_\infty = \tan^{-1} \frac{c_a}{u - \frac{\Delta c_u}{2}} \tag{2.2b}$$

For IGV (c/) case:

$$w_\infty^2 = c_a^2 + \left(u + \frac{\Delta c_u}{2}\right)^2 \tag{2.3a}$$

and

$$\beta_\infty = \tan^{-1} \frac{c_a}{u + \frac{\Delta c_u}{2}} \tag{2.3b}$$

$w_\infty$ :   relative free-stream (undisturbed) flow velocity

$\beta_\infty$ :   free-stream flow angle

The rotor blade row is a decelerating blade row: the outlet relative velocity is lower than the inlet one. In such a "diffuser-like" flow, special attention is to be paid to the risk of flow separation (stall).

The OGV is also a decelerating cascade: the outlet absolute velocity is lower than the inlet one. In this "diffuser-like" flow, the extra dynamic pressure due to swirl is converted to static pressure rise by reducing the outlet swirl. The OGV is to be checked in design in order to avoid flow separation (stall). Due to the OGV, the static pressure rise by the rotor is reduced. The reaction degree is defined as follows:

$$\tau = \Delta p_{st} \, / \, \Delta p_{t, \, rotor} \tag{2.4}$$

Since the OGV eliminates the outlet swirl, and the inlet and outlet axial velocities are equal due to the identical inlet and outlet annular flow cross-sections, the total pressure rise due to the rotor is equal to the static pressure rise (measured static pressure difference) due to the rotor + OGV configuration (i.e. the fan stage).

For rotor + OGV configuration:

$$\tau = (\Delta p_{st \, rotor} + \Delta p_{st \, OGV}) / \Delta p_{st \, stage} \tag{2.5}$$

Pointing out that the reaction degree is less than 1 when applying OGV.

Using IGV, the guide vane is an accelerating cascade: the outlet absolute velocity is higher than the inlet one. In such a "confuser-like" flow, no risk of separation occurs (that is why the IGV blades can be manufactured from sheet metal in the case of fans of moderate size). However, the acceleration by the IGV leads to pressure decrease. Therefore, the static pressure rise on the rotor must be higher than the total pressure rise.

For IGV + rotor configuration:

$$\tau = (\Delta p_{st \, rotor} - \Delta p_{st \, IGV}) / \Delta p_{st \, stage} \tag{2.6}$$

Pointing out that the rotor reaction degree is higher than 1 when applying an IGV. It must also be noted that $w_\infty$ also increases in this case, which means that increased total pressure rise can be realised with a fixed rotor circumferential speed. (In other words: although the static pressure rise on the rotor is higher when using an IGV, the related diffuser effect is still moderate due to the increased relative velocity through the rotor.)

## 2.3. Operation of the blade sections. Work equation of the elemental rotor cascade.
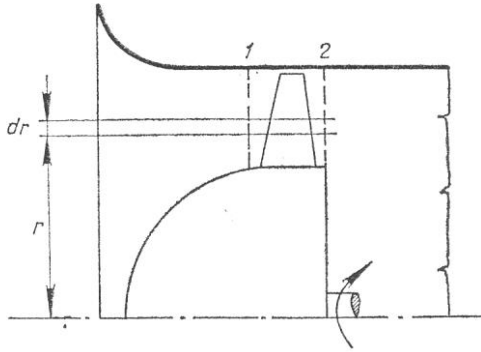


***Fig. 2.12. Selection of an elemental rotor cascade in an isolated (vaneless) rotor [2]***

Cylindrical stream tubes are assumed through the rotor. An elemental stream tube enclosing an elemental rotor blade cascade is under discussion (Fig. 2.12).

The angular momentum equation is applied to the air quantity bounded by the cylindrical stream surfaces of radius r and (r + dr) as well as by the „1" (rotor inlet) and the „2" (rotor outlet) planes. The torque coming from the shear forces appearing on the cylindrical surfaces are neglected. The result is

$$dq_m \, r \, \Delta c_u = \rho \, 2 \, \pi \, r \, dr \, c_a \, r \, \Delta c_u = dM \qquad (2.7)$$

Indicating that the product of elemental mass flow rate and change of angular momentum of the air is in relationship with the elemental torque expressed on the air mass by the elemental rotor.

On the other hand, the elemental torque $dM$ can also be expressed with use of elemental forces acting on the elemental blades. **Fig. 2.13.** The inlet and outlet relative velocities and their vectorial mean – corresponding to $w_\infty$ – are derived. The blade element must be staggered at an angle of attack (incidence angle) $\alpha$ relative to the direction of the free-stream velocity to provide an elemental lift force $dF_L$ necessary for production of the prescribed total pressure rise $\Delta p_t$ .

The elemental blade force $dF_r$ has a lift force component $dF_L$ normal to $\underline{w}_\infty$ and has a drag force component $dF_D$ parallel with $\underline{w}_\infty$ . The relationship of these elemental forces is

$$\frac{dF_D}{dF_L} = \frac{c_D}{c_L} = \tan \delta \qquad (2.8)$$

Being the reciprocal value of the lift-to-drag ratio. $c_D$ and $c_L$ are the drag and lift coefficients of the blade section. For example, the lift force is

$$dF_L = \frac{\rho}{2} w_\infty^2 \, ldr \, c_L \qquad (2.9)$$

Since $dF_D$ is much smaller than $dF_L$ , $|dF_L| \approx |dF_r|$, the torque reacting on the blade element is

$$dM = N \, r \, dF_r \, \sin(\beta_\infty + \delta) \approx N \, r \, \frac{\rho}{2} w_\infty^2 \, ldr \, c_L \, \sin(\beta_\infty + \delta) \qquad (2.10)$$
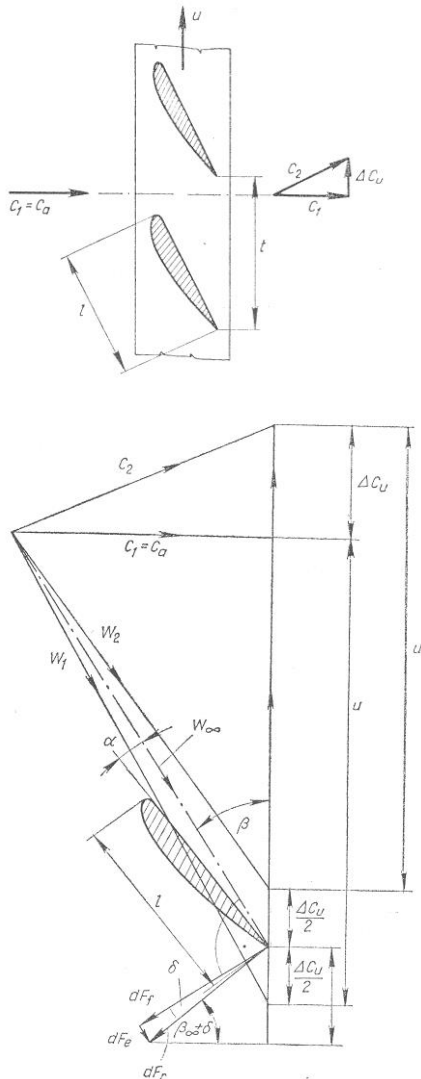
Where $N$ is the blade count.

Making Eqs. (2.7) and (2.10) equal, and introducing the blade pitch

$$t = \frac{2\pi r}{N}$$

(2.11)

The so-called **force factor** $\frac{1}{t}c_L$ can be expressed:

$$\frac{1}{t}c_L = \frac{2\,c_a \Delta c_u}{w_\infty^2 \sin(\beta_\infty + \delta)}$$

(2.12)

This is the **work equation** of the elemental cascade.



***Fig. 2.13. Aerodynamic characteristics of an elemental blade section  [2]***

At the present level of discussion, the following approximation is applied, considering that $\delta \ll \beta_\infty$:

$$\frac{1}{t}c_L \approx \frac{2\,c_a \Delta c_u}{w_\infty^2 \sin\beta_\infty} = \frac{2\,\Delta c_u}{w_\infty}$$

(2.13)

It is clear that the work equation reflects how the operational demands ($\Delta c_u$, $w_\infty$) can be realised with an elemental blade cascade of appropriate characteristics ($c_L$, $\dfrac{1}{t}$ so-called **solidity**).

**EXAMPLE: classic design method: design for spanwise (in radial direction) constant $\Delta p_t$ total pressure rise.** This also results in spanwise constant axial velocity if the inlet axial velocity is uniform.

If the circumferential speed $u$ is selected, $\Delta c_u$ can be calculated from the demanded design $\Delta p_t$ value, using the Euler equation of turbomachinery, and using an estimate for the hydraulic efficiency:

$$\Delta c_u = \frac{\Delta p_t}{\eta_h \rho u} \tag{2.14}$$

The $c_a$ axial velocity can be calculated from the volume flow rate $q_v$ if the hub and tip diameters are defined by the designer:

$$c_a = \frac{4\, q_v}{(D^2 - d^2)\, \pi} \tag{2.15}$$

Based on the above, $w_\infty$ can be calculated:

$$w_\infty = \sqrt{c_a^2 + \left(u - \frac{\Delta c_u}{2}\right)^2} \tag{2.16}$$

Therefore, the data necessary for calculation of the force factor (Eq. (2.13)) are available.

## 2.4. Principles of blade design

The following example follows one possible principle (used at the Dept. of Fluid Mechanics, BME, following the British design traditions) e.g. for design of an isolated (vaneless) rotor. Several methods exist worldwide, depending on the related experimental database. E. g. USA: based on NACA profile measurements etc.

1/      Prescribed design conditions: mean $\Delta p_t$ , and $q_v$ .

2/      The rotor outer diameter, the rotor speed, and the hub-to-tip ratio are prescribed on the basis of design experiences, supported by literature data (e.g. Cordier diagram).

3/      The spanwise (radial) distribution of ideal total pressure rise must be prescribed. As shown later, this also determines the spanwise distribution of the axial velocity. With appropriate estimation of mean hydraulic efficiency, these distributions must result in the mean design characteristics: $\Delta p_t$ , and $q_v$ .

Example: in classic design, for spanwise constant ideal total pressure rise (no IGV, $\Delta c_u = c_{u2}$):

$$\Delta p_t(r) = const = \rho\, u\, \Delta c_u(r) = \rho\, u\, c_{u2}(r) \tag{2.17}$$

Since $u$ increases linearly with radius, $c_{u2}$ must decrease hyperbolically with radius:

$$c_{u2}(r) = \frac{\Delta p_t}{\rho\, \omega}\, \frac{1}{r} \tag{2.18}$$

This spanwise hyperbolically decreasing distribution of tangential velocity corresponds to that of a potential vortex, also termed as "free vortex". On this basis, this design method is referred to as **Free Vortex Design**.

It will be shown later that the free-vortex design results in spanwise constant axial velocity in the annulus, if the rotor inlet axial velocity is constant. Therefore,

$$c_a = \frac{4\,q_v}{(D^2 - d^2)\pi} \tag{2.19}$$

4/      The blading is divided to elemental rotors. The force factor $\frac{1}{t}c_L$ is calculated for each elemental rotor, with knowledge of local $u$, $c_{u2}$ (Eq. 2.18) and $c_a$ (Eq. 2.19) data, on the basis of Eqs. (2.13) and (2.16).

5/      An empirical database is selected for the shape optimisation of the individual blade sections comprising the elemental rotors. For example, **Fig. 2.14** shows the two-dimensional (2D) measurement data on a classic airfoil (RAF 6) in isolated (single airfoil, no cascade) arrangement. (Other ways: cambered plate measurements, other profiles, cascade measurements, etc…)

6/      The "optimum" value of $c_L$ is selected in an energetically optimum manner: the machine should give the highest efficiency. It can be pointed out that this can be achieved at the maximum lift-to-drag ratio. This will define the incidence angle $\alpha$ as well, at which the blade section must be aligned relative to the free-stream velocity direction.

7/      From the optimum $c_L$ and from the $\frac{1}{t}c_L$ data, optimum solidity $\frac{1}{t}$ is calculated. It must be checked if the result is consistent with the selected empirical database. For example, using Fig. 2.14, if the computed $\frac{1}{t}$ is "too high" (above 0.7), the interaction between the neighbouring blades cannot be neglected and it is not true that the individual blade section can be considered as an "isolated" one. In this case, a compromise is to be made: either the value of $c_L$ must be modified, or other empirical databases (e.g. cascade data) are to be used.

8/      The *N* blade count is defined. Blades of low number with high chord length are beneficial (higher Reynolds number).

9/      From the optimum value for $\frac{1}{t}$, the chord length *l* necessary at the given radius is calculated. The geometrical data *l*, ($\beta_\infty + \alpha$) and knowledge regarding the profile shape at each elemental rotor radius defines the shape of the blades.
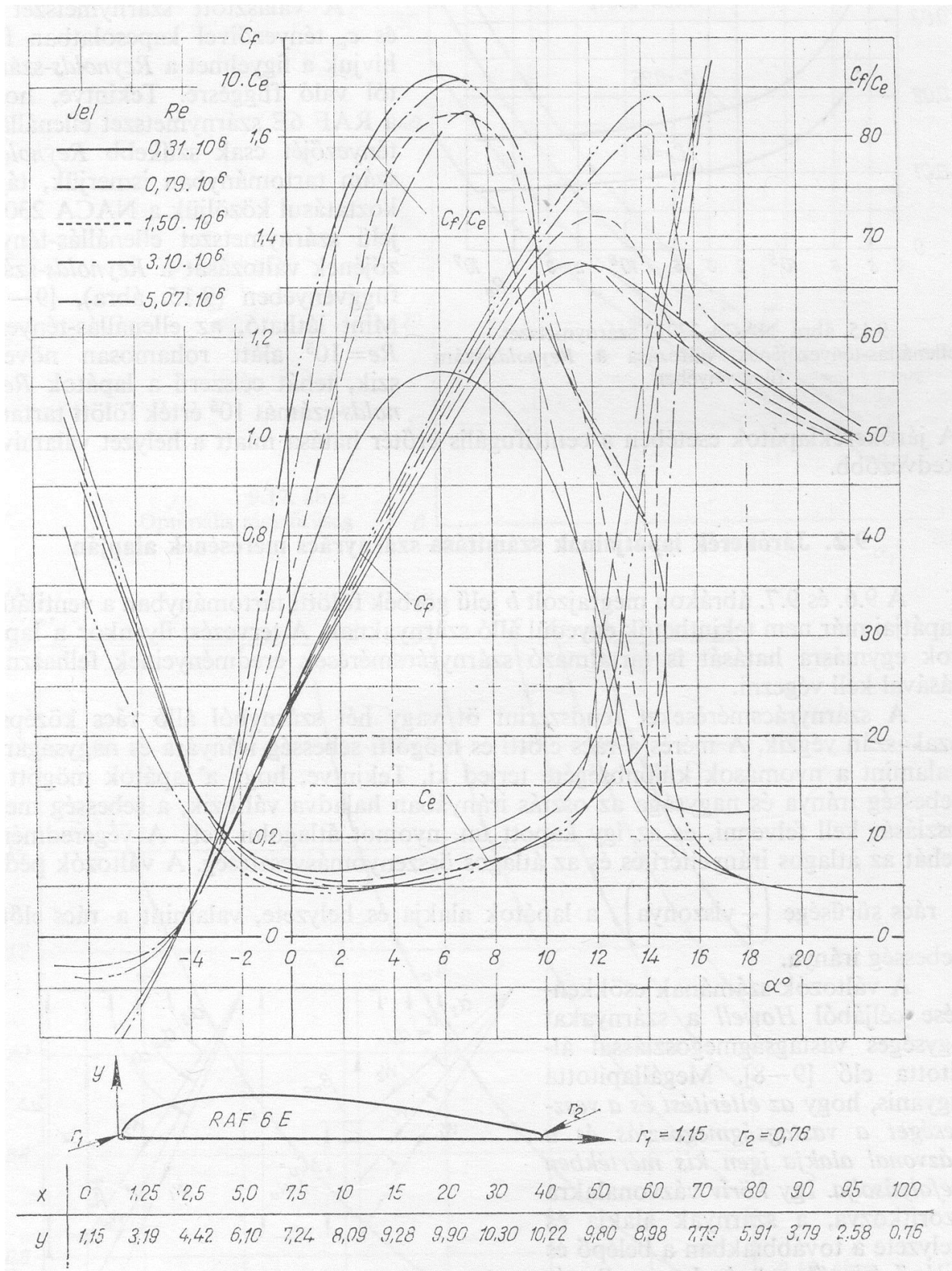
*Fig. 2.14. Coordinates and force coefficients of RAF 6E profile (isolated 2D airfoil)  [2]*